An adaptive characteristics method for advective-diffusive transport

Ouyang Zhihua

Department of Mining Engineering, Wuhan Steel and Iron University, People's Republic of China

Derek Elsworth*

Department of Mineral Engineering, Pennsylvania State University, University Park, PA, USA

An adaptive characteristics method is presented for the solution of advective-diffusive groundwater transport problems. The method decomposes the transport processes into advective and diffusive transport components. Advective flows are defined by using a streamtube incrementing procedure, based on the method of characteristics, to define the position of the advective front. Diffusive transport orthogonal to the front is represented by an array of propagating streamtube elements, with dimension determined from analytical solution of the one-dimensional diffusion equation. Adaptive time scaling is used to moderate the dimensions and aspect ratios of the advective and diffusive streamtube elements as appropriate to the dominant transport mechanism. Finite differences are used to solve for transport ahead of the advancing front. The distribution of streamtubes are predetermined from a direct boundary element algorithm. Comparison with analytical results for a one-dimensional transport geometry indicates agreement for Peclet numbers between zero and infinity. Solution for transport in two-dimensional domains illustrates excellent agreement for Peclet numbers from zero to 25.

Keywords: advective-diffusive transport, characteristics, numerical methods, groundwater transport

Introduction

A variety of numerical methods have been proposed to allow effective solution of advective-diffusive transport phenomena. Of particular concern is the behavior of Eulerian-based methods in which advective flows dominate and the governing equations become hyperbolic. Related problems of oscillatory behavior and overshoot surrounding steep concentration gradients may be accommodated by using upwind techniques;[1] however, numerical diffusion of unknown magnitude is introduced as a natural consequence. The method of characteristics[2] is a powerful technique when applied to differential equations exhibiting significant first-order derivatives and has been applied to the solution of density-dependent[3] and density-independent[4,5] transport problems. Adaptive methods incorporating mixed Eulerian-Lagrangian techniques[6,7] have been used to retain the most effective attributes of the respective methods in representing a broad range of both advection-dominated and diffusion-dominated flows.

The proposed method is an extension of the coupled finite element and characteristics schemes employed in the solution of the full Navier-Stokes equations. Their common form requires that the advective term $\partial\rho/\partial t + v\cdot\nabla\rho$, representing conservation of mass along a streamline, is treated as a total derivative $D\rho/Dt$ and solved by using the method of characteristics. In an analogous manner, mass concentration may be substituted for density, ρ, used in the Navier-Stokes problem to parallel the mass transport of a single species. In the methods introduced by Benque et al.[8] and developed by others[9–11], diffusive transport is represented by finite difference or Galerkin finite element methods in which stability of the solution is guaranteed. The robustness and attractive stability characteristics of these operator-splitting techniques have consequently attained wide appeal. Our method differs from previous ones in the application of an analytical kernel to represent progression in the dispersive flux via a migrating Lagrangian element assemblage.

*Currently at Waterloo Centre for Groundwater Research, University of Waterloo, Waterloo, Canada.

Address reprint requests to Dr. Elsworth at the Department of Mineral Engineering, Pennsylvania State University, 116 Mineral Sciences Building, University Park, PA 16802, USA.

Received 21 September 1988; accepted 20 July 1989

An adaptive characteristics method is presented in the following for solution of a broad category of advection- and diffusion-dominated transport problems utilizing a streamtube element. The streamline method reduces problems of mesh tangling inherent within Lagrangian methods, allowing general and flexible application to a wide variety of problem types involving straightforward coupling of flow and transport behavior. A boundary element method is used to solve for streamtube geometries within the flow domain, and a method of adaptive characteristics solves the advection-diffusion equation. As a consequence of the property of constant discharge within a single streamtube, the advective component of the steep concentration front is tracked forward with the aid of a moving streamline-element. In advance of the front, the size of the element is determined by a new criterion allowing effective element sizing and time step sequencing in one- and two-dimensional transient transport problems.

Theory

The appropriate partial differential equation that governs the transport of a conservative substance in a two-dimensional flow field can be written in the form

$$\frac{\partial C}{\partial t} = \frac{\partial}{\partial x_i}\left(D_{ij}\frac{\partial C}{\partial x_j}\right) - v_i\frac{\partial C}{\partial x_i} \qquad i,j = 1,2 \tag{1}$$

where C = concentration of the dissolved chemical species, M/L^3
v_i = seepage velocity in the direction of x_i, L/T
t = time variable, T
D_{ij} = hydrodynamic dispersion tensor, L^2/T

Initial data specify the concentration everywhere in the solution region, Ω, as illustrated in *Figure 1* as

$$C_0(x_1, x_2) = C(x_1, x_2, t_0) \qquad \text{at} \quad t = t_0 \quad \text{on}\,\Omega \tag{2}$$

Two boundary conditions are applied to (1) to specify the concentration on a part of the boundary, Γ_1 (the Dirichlet condition),

$$C_1 = C(x_1, x_2, t) \qquad \text{on}\,\Gamma_1 \tag{3}$$

and to specify the normal gradient of the concentration on the remainder of the boundary, Γ_2, shown in *Figure 1* (the Neumann condition),

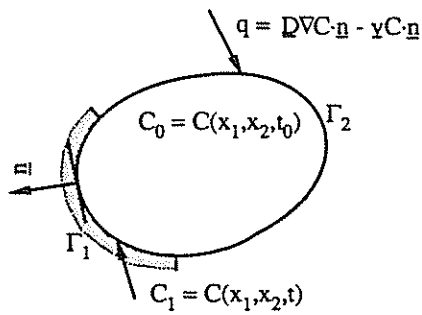

Figure 1. Solution domain with boundary and initial conditions

$$q = \mathbf{D}\nabla C\cdot\mathbf{n} - \mathbf{v}C\cdot\mathbf{n} \qquad \text{on}\,\Gamma_2 \tag{4}$$

where ∇ is the gradient operator $(\partial/\partial x, \partial/\partial y)$, $\mathbf{v}$ is the seepage velocity vector, $\mathbf{D}$ is the diffusion tensor, and $\mathbf{n}$ is outward unit normal to the boundary. An additional mixed condition represents a combination of (3) and (4). The approach taken by the method of characteristics is not to solve equation (1) directly, but rather to solve an equivalent system of ordinary differential equations.

In the general case the dispersion coefficient D_{ij}, comprising the components of $\mathbf{D}$ in (4), may be related to the velocity of groundwater flow and to the nature of the aquifer using Scheidegger's[12] equation:

$$D_{ij} = \alpha_{ij\xi\zeta}\frac{v_\xi v_\zeta}{|\mathbf{v}|} \tag{5}$$

where $\alpha_{ij\xi\zeta}$ = dispersivity of the aquifer, L
v_ξ and v_ζ = components of velocity in the ξ- and ζ-directions, respectively, L/T
$|\mathbf{v}|$ = magnitude of velocity, L/T

Where consideration is restricted to the longitudinal and transverse directions of flow, the dispersivity tensor may be recorded in principal form, using the longitudinal and transverse dispersivities of the aquifer. Where subscripts s and n refer to the streamline and normal to streamline directions, respectively, the longitudinal and transverse dispersion coefficients are given by

$$D_{ss} = D_{11} = \alpha_L|v_s| \tag{6}$$

$$D_{nn} = D_{22} = \alpha_T|v_s| \tag{7}$$

$$D_{ij} = 0 \qquad \text{for}\; i \neq j \tag{8}$$

where v_s = velocity of flow direction, L/T
α_L = longitudinal dispersivity of the aquifer, L
α_T = transverse dispersivity of the aquifer, L

Along an individual streamline, equation (1) may be rewritten as

$$\frac{\partial C}{\partial t} = \frac{\partial}{\partial s}\left(D_{ss}\frac{\partial C}{\partial s}\right) + \frac{\partial}{\partial n}\left(D_{nn}\frac{\partial C}{\partial n}\right) - v_s\frac{\partial C}{\partial s} - v_n\frac{\partial C}{\partial n} \tag{9}$$

Representative fluid particles and streamline elements may be defined that are advected with the flowing groundwater. Transient changes in the properties of the fluid, such as concentration, may be described either for fixed points within a stationary coordinate system as successive fluid particles pass the reference points or for reference fluid particles as they move along their respective paths past fixed points in space. Associated with these two descriptions are two derivatives with respect to time. The rate of change of concentration as observed from a fixed point is defined as $\partial C/\partial t$, whereas the material derivative,[13] dC/dt, is the rate of change as observed when moving with the fluid particle.

The material derivative of concentration may be defined as

$$\frac{dC}{dt} = \frac{\partial C}{\partial t} + \frac{\partial C}{\partial s}\frac{ds}{dt} + \frac{\partial C}{\partial n}\frac{dn}{dt} \tag{10}$$

Comparing (10) with (9) yields

$$\frac{ds}{dt} = v_s \qquad \frac{dn}{dt} = v_n \tag{11a}$$

and since, by definition, no flow can cross a streamline, the velocity v_n normal to the flow direction must be zero. In the cartesian coordinate system,

$$\frac{dx}{dt} = v_x \qquad \frac{dy}{dt} = v_y \tag{11b}$$

and (9) therefore possesses a single characteristic, along which (9) reduces to

$$\frac{dC}{dt} = \frac{\partial}{\partial s}\left(D_{ss}\frac{\partial C}{\partial s}\right) + \frac{\partial}{\partial n}\left(D_{nn}\frac{\partial C}{\partial n}\right) \tag{12}$$

and solutions to the system of equations comprising (11) may be given as

$$s = s(t) \quad n = \text{constant} \quad \text{and} \quad C = C(t) \tag{13}$$

Solution to the system of equations (11)–(12) is developed through application of an adaptive streamline element.

A streamline is everywhere tangent to the seepage velocity vector (or the specific discharge vector), **v**, with adjacent streamlines comprising individual streamtubes. Since, by definition, no flow can cross a streamline, the flow rate along a streamtube is constant, provided that steady conditions prevail and that no distributed sources and sinks exist in the flow domain. By the above definition the equation of a streamline is

$$\mathbf{v} \times \mathbf{ds} = 0 \tag{14a}$$

where × denotes a cross product and **ds** is the element vector along the streamline as illustrated in *Figure 2(a)*. In cartesian coordinates, (14) may be written as

$$v_y dx - v_x dy = 0 \tag{14b}$$

We can now define a stream function, or Lagrange stream function, $\Psi = \Psi(x, y)$ that is constant along a streamline, and hence

$$d\Psi = \frac{\partial \Psi}{\partial x}dx + \frac{\partial \Psi}{\partial y}dy = 0 \tag{15}$$

By comparing (14) in component form with (15) we find that

$$v_x = -\frac{\partial \Psi}{\partial y} \qquad v_y = \frac{\partial \Psi}{\partial x} \tag{16}$$

The physical interpretation of Ψ may be obtained by considering the integral of Ψ between two points on the adjacent streamlines, say a and b in *Figure 2(b)*.

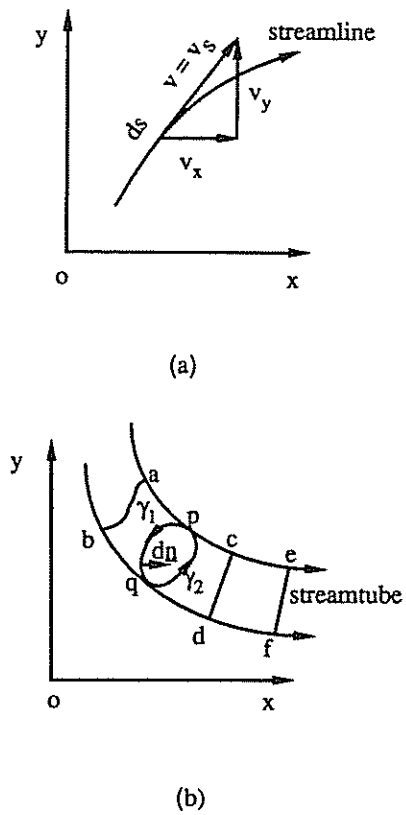

Figure 2. Cartesian space containing (a) streamlines and (b) streamtubes

If we consider the two integrals in *Figure 2(b)*,

$$\int_p^q \mathbf{v}\cdot d\mathbf{n} = \int_q^p \mathbf{v}\cdot d\mathbf{n} \tag{17}$$

then (17) holds for steady incompressible flow in the absence of sources and sinks. The integral of (17) is path-independent, and accordingly, we may choose any path between points a and b. Since the differential of $\Psi_b - \Psi_a$ depends only on the endpoints of the integration, the total flow through the streamtube ΔQ_{ab} is given by

$$\begin{aligned}\Delta Q_{ab} &= \int_a^b \mathbf{v}\cdot d\mathbf{n} = \int_a^b (v_x dy - v_y dx) \\ &= \int_a^b -\frac{\partial \Psi}{\partial y}dy - \frac{\partial \Psi}{\partial x}dx \\ &= -\int_a^b d\Psi = \Psi_a - \Psi_b\end{aligned} \tag{18}$$

Hence the total discharge (in terms of volume per unit width normal to the xy-plane per unit time) between two streamlines is equal to the difference in the stream functions corresponding to these lines. If points

a and b are on the same streamline, $\Delta Q_{ab} = 0$, $d\Psi = 0$, and ψ = constant.

As a special example, let us consider the rectangular $cdfe$ (see *Figure 2(b)*) between the two adjacent streamlines. Because the paths ce and df are on the streamlines, the integrals on these segments are equal to zero. Therefore the eventual integral becomes

$$\int_c^d \mathbf{v}\cdot d\mathbf{n} = \int_e^f \mathbf{v}\cdot d\mathbf{n} \tag{19}$$

namely, the total discharge through any section in the same streamtube is constant. We can now define a streamline element. As illustrated in *Figure 3(a)*, we assume that there are some tracking points corresponding to the streamlines at time level $k-1$ (for example, points a, b, c, d, e, and f), and they are distributed by the separation

$$\Delta s_{bd} = v_{bs}\Delta t \qquad \Delta s_{df} = v_{ds}\Delta t \tag{20}$$

where Δs_{bd} and Δs_{df} are the distances between points b, d and d, f, respectively, along the streamlines; Δn_{ab} and Δn_{ef} are the span between appropriate points on the adjacent streamlines; v_{bs} and v_{ds} are velocities in the flow direction (i.e., specific discharges) at points b and d; and Δt is the time increment. The rectangular domains $abdc$ and $cdfe$ are defined as streamline elements and exhibit two specific properties. First, the areas of all the streamline elements are identical for a constant time increment Δt such that

$$A_{abdc} = \Delta t \int_a^b \mathbf{v}\cdot d\mathbf{n} = \Delta t \int_c^d \mathbf{v}\cdot d\mathbf{n} = A_{cdfe} \tag{21}$$

where A_{abdc} and A_{cdfe} are the areas of the streamline elements (L^2). Second, as shown in *Figure 3(b)*, the streamline elements are controlled by the migration of tracking particles attached directly to the streamlines. The advective distance travelled in the time increment Δt for each of the streamline elements is the length of a streamline element. For example, the element $cdfe$ in *Figure 3(b)* was advected to a new position at time level k. Hence the replacement element $abdc$ migrates to the previous location of element $cdfe$ at time level $k-1$. The solute concentration in each of the elements is therefore constant in transport caused by advection alone. As a result, the computational burden in evaluating transient concentration changes is eased over general particle tracking methods[1-4] without loss in precision.

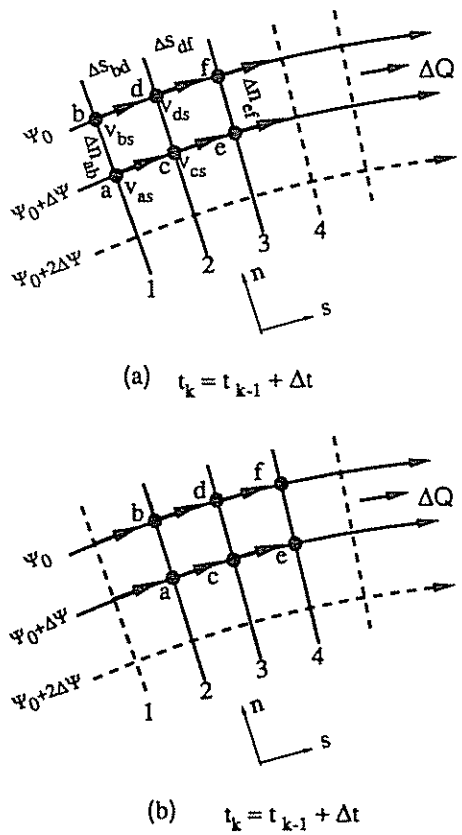

Figure 3. Streamline elements and grids at successive time levels illustrating migration

Numerical method

The proposed numerical procedure involves the decomposition of the transport process into the two component parts: advection and diffusion.[7,8] The solution of the transport equation thus reduces to solving the system of equations represented by (11) and (12). In the general case, three main steps will be adopted in each time step of the numerical computation. The first step is to generate a streamline element caused by advective transport alone; the second step is to generate a streamline element caused by diffusive transport alone; and the final step utilizes finite difference approximations to calculate the concentration change represented in (12).

Advective transport

Equations (11) are solved by first placing a number of particles or points along the boundary of the concentration sources, for example, particles a_0, b_0, and c_0 and then tracking the movement of these particles as illustrated in *Figure 4*. A uniformly spaced stream of particles is maintained by generating a new particle at the same relative position because particle movement is governed by equation (11). Point a_0 at $t = t_0$ (*Figure 4(a)*) was advected to a new position (*Figure 4(b)*) after time increment Δt. Because transport is caused by advection alone, the concentration is equal to C_0 behind the front. The replacement point a_1 is placed at the location of point a_0 at $t = t_0$. Because each of the particles migrates along a streamline, we may use this information and the properties of a streamline to calculate the change in concentration. The first streamline element in streamtube i can be defined by four adjacent points, for example, a_1, a_0, b_0, and b_1 in *Figure 4(b)*. At time t_k we have k streamline elements generated by pure convection in the ith streamtube as illustrated in *Figure 4(c)*.

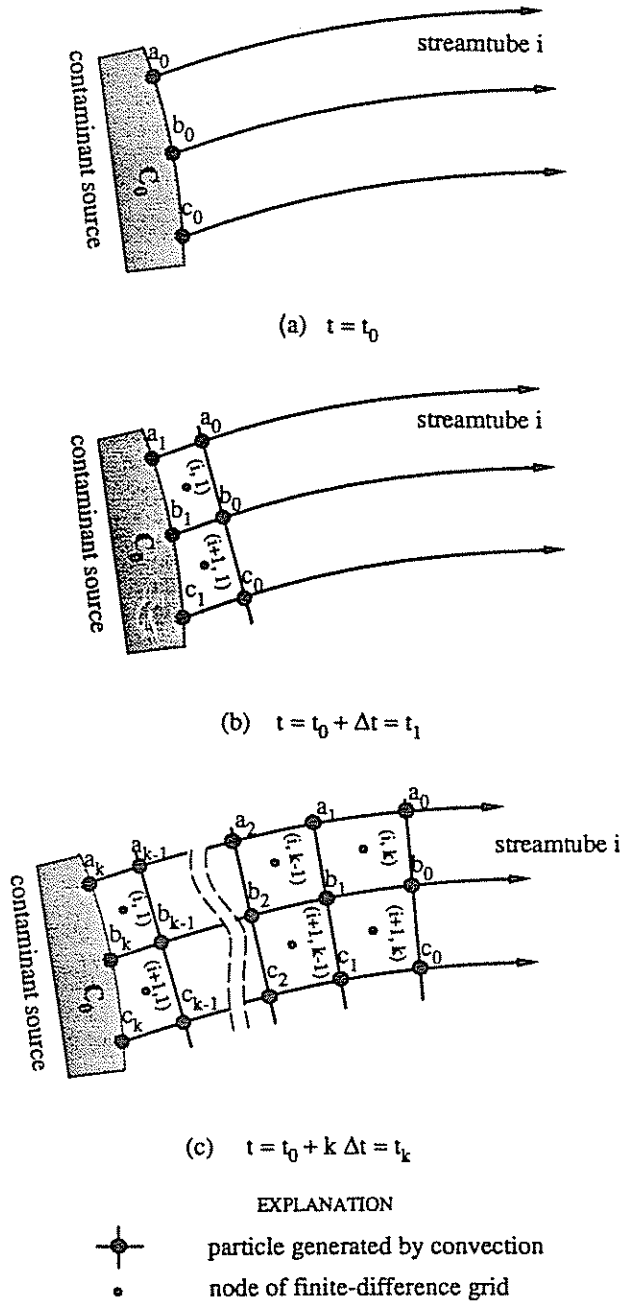

Figure 4. Particle tracking method applied along streamlines

The four sides of any streamline element are parallel to the axes of the local $(s - n)$ coordinate system. The finite difference grid for (12) therefore coincides with the sides of streamline elements, the nodes of the grid representing the center points of streamline elements. The difference between the nodes and the center points is that the nodes of a finite difference grid are fixed, whereas the center points of streamline elements will move with time. In numerical computations the concentration distribution in the domain of interest will be known at any time level k because of the properties of the streamline elements. For convenience the numerical computation at time level k will be completed only in the area directly ahead of the concentration front. Note that in *Figure 4* we use notation (i,j) to indicate the node of the finite difference grid, where i represents the ith streamtube and j represents the jth node of the finite difference grid. At any time level k the concentration in the element (i,j) may be denoted as $C_{i,j,k}$, also representing the concentration in an appropriate whole streamline element. When $t = t_1$, the first row of streamline elements is generated, and the contaminant concentration at the node $(i, 1)$ or in the appropriate element is simply given as $C_{i,j,k} = C_0$ because of purely advective transport (see *Figure 4(b)*). Under similar reasoning, the second row of streamline elements $(i, 2)$ with concentration C_0 is generated at time t_2 and occupies the same position in which the first elements were at time t_1. Under pure advection the concentration in all the elements is given by $C_{i,j,k} = C_0$ when $t = t_k$. As a result, the interface a_0, b_0, c_0 in *Figure 4* is abrupt.

For each time step, every particle is moved a distance proportional to the product of the time increment and the velocity at the location of the particle. The new position of a particle is thus computed with the finite difference forms of (11) as

$$x_{p,k} = x_{p,k-1} + \Delta x_p = x_{p,k-1} + \Delta t\, v_{x[x(p,k),y(p,k)]} \tag{22}$$

and

$$y_{p,k} = y_{p,k-1} + \Delta y_p = y_{p,k-1} + \Delta t\, v_{y[x(p,k),y(p,k)]} \tag{23}$$

where p is the index number for particle identification and Δx_p and Δy_p are the distances moved in the x- and y-directions, respectively. The x and y velocities at the position of any particle p, indicated as $v_{i[x(p,k),y(p,k)]}$, for the time level k are calculated through use of a direct boundary element method[15] with a streamline tracking facility. The locations of all streamline elements are known following the incrementing procedure identified previously. In the general case of mixed advective-diffusive transport the concentration at each node or streamline element is denoted as $C^*_{i,j,k}$ at time level k prior to modification for diffusive spreading. The time index is distinguished with an asterisk, since the temporary concentration at time level k is defined only with respect to advective transport. Because of the properties of a streamline element, it follows directly that

$$C^*_{i,j,k} = C_{i,j-1,k-1} \tag{24}$$

In pure advection the interface a_0, b_0, c_0 of *Figure 4* advances in time with the area ahead of the front retaining a null concentration. This demarcation negates the meshing of streamline elements in the zone ahead of the concentration front.

Dispersive transport

Dispersion causes both longitudinal and transverse spreading, the latter propagating beyond the streamtube boundaries. The length to which longitudinal

spreading occurs ahead of the sharp advective front is conditioned by the time increment Δt as illustrated in *Figure 5(a)*. Considering a single streamtube comprising the domain, Ω, as illustrated in *Figure 5(b)*, a streamtube element representing dispersive transport must be generated. When dispersion is neglected, an abrupt transition exists between the two zones where concentration levels are $C = C^*_{i,j,k}$ at node (i,j) and $C = 0$ ahead of this location. Based on the solution for constant hydraulic flux in the $+s$-direction, the concentration distribution ahead of the front is given[16] as

$$C(\Delta s_d, \Delta t) = \frac{C^*_{i,j,k}}{2} \operatorname{erfc}\left[\frac{\Delta s_d}{(4D_{ss}\Delta t)^{0.5}}\right] \tag{25}$$

where Δs_d = longitudinal spreading length
Δt = time increment
$C^*_{i,j,k}$ = temporary concentration at node (i,j) before longitudinal spreading due to dispersion at time level k

$$\operatorname{erfc}(\theta) = 1 - \operatorname{erf}(\theta) = \frac{2}{\sqrt{\pi}} \int_{\theta}^{\infty} e^{-\beta^2}\, d\beta$$

$$\theta = \frac{\Delta s_d}{(4D_{ss}\Delta t)^{0.5}}$$

If we set $\lambda = \theta\sqrt{2}$ and $\omega = \sqrt{2}\beta$, then $d\omega = \sqrt{2}d\beta$, and (25) reduces to

$$\begin{aligned} C(\Delta s_d, \Delta t) &= \frac{C^*_{i,j,k}\sqrt{2}}{\sqrt{\pi}} \int_{\lambda}^{\infty} e^{-\omega^2/2}\, d\omega \\ &= 2C^*_{i,j,k}\left[1 - \frac{1}{\sqrt{2\pi}} \int_{-\infty}^{\lambda} e^{-\omega^2/2}\, d\omega\right] \\ &= 2C^*_{i,j,k}[1 - \operatorname{prob}(Z \le \lambda)] \end{aligned} \tag{26}$$

which describes a normal distribution perpendicular to the interface of *Figure 5(b)*. In (26) the function prob $(Z \le \lambda)$ is the normal probability function. If we prescribe the concentration at some distance ahead of the dispersive front to be zero, then

$$C(\Delta s_d, \Delta t) = 2C^*_{i,j,k}[1 - \operatorname{prob}(Z \le \lambda)] = 0 \tag{27}$$

Although $C(\Delta s_d, \Delta t)$ becomes zero only when λ becomes infinite, computational expedience requires that a specific value of λ be chosen merely to meet precision requirements. Accordingly, if $\lambda = 3.0$, then prob $(Z \le 3.0) \simeq 0.998650$, or if $\lambda = 4.0$, prob $(Z \le 4.0) \simeq 0.99996833$. Effectively, therefore, for $\lambda \ge 3.0$ the magnitude of $C(\Delta s_d, \Delta t)$ is approximately equal to zero. Later results indicate that the factor λ has little influence on the numerical calculation. From the above discussion we obtain

$$\Delta s^*_d = \lambda\sqrt{2D_{ss}\Delta t} \tag{28}$$

where λ is the prescribed value of $\theta\sqrt{2}$ and Δs^*_d is the longitudinal size of a streamline element caused by dispersion only. When the time increment Δt is prescribed, the magnitude of Δs^*_d is known, and thus a

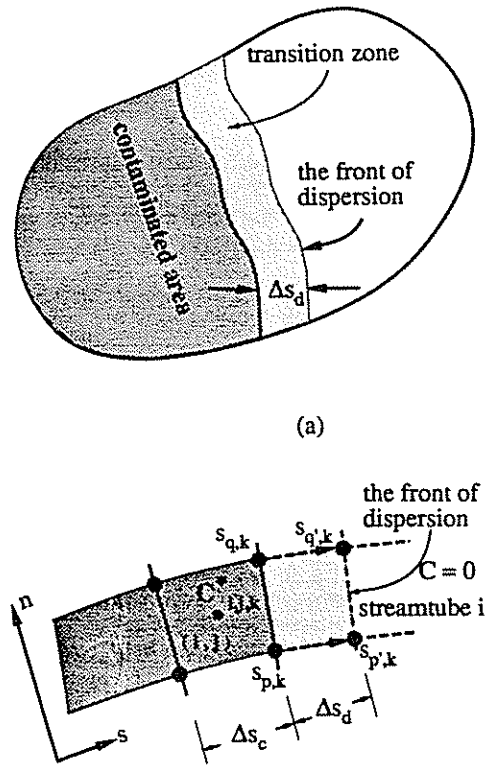

Figure 5. Advective and dispersive transport mechanisms shown (a) schematically and (b) for dispersive streamline elements

streamline element resulting from diffusion alone is generated. New particles p' (and q') are created at p (and q) of *Figure 5* and are moved ahead by a migration length Δs^*_d. The migration increment is evaluated from the finite difference form of (11) as

$$s_{p',k} = S_{p,k} + \Delta s^*_d = S_{p,k} + \lambda\sqrt{2D_{ss}\Delta t} \tag{29}$$

Particle p' is moved from position $s_{p,k}$ to position $s_{p',k}$ in the time increment, and the streamline element at node $(i, j + 1)$, caused by dispersion alone, is determined by the particles $s_{q,k}$, $s_{q',k}$, $s_{p,k}$, and $s_{p',k}$ at time level k. The concentration in the element of node $(i, j + 1)$ remains zero and will be calculated by the formula in the following section.

From (6) and (28) the lengths of the elements representing diffusive (Δs^*_d) and advective (Δs_c) transport are related as

$$\begin{aligned} \Delta s^*_d &= \lambda\sqrt{2D_{ss}\Delta t} = \lambda\sqrt{2|v_s|\Delta t} \\ &= \lambda\sqrt{2(\Delta x^2 + \Delta y^2)} = \lambda\sqrt{2}\Delta s_c \end{aligned} \tag{30}$$

or

$$\frac{(\Delta s_d^*)^2}{\Delta s_c} = \lambda\sqrt{2} \tag{31}$$

where Δs_c is the longitudinal size of the element caused by advective transport only. In (30) and (31) the relationship between Δs_d^* and Δs_c is quadratic. If the time increment Δt is chosen a priori, the sizes of these two kinds of elements (Δs_d^* and Δs_c) are fixed. To avoid problems of numerical diffusion resulting from inappropriate size ratios within the streamline elements generated by both advection and diffusion, the travel distance increments Δs_d^* and Δs_c (i.e., streamline element length) in these two equations are given an identical value, Δs. From (6) and (30) we have

$$\Delta t_c = \frac{\Delta s}{vs} \qquad \Delta t_d = \frac{(\Delta s)^2}{2\lambda^2 D_{ss}} \tag{32}$$

with the result that the time increment used in the computation is conditioned by the dominant transport mode. Accordingly,

$$\Delta t = \Delta t_c \qquad \text{if } \Delta t_d > \Delta t_c$$
$$\Delta t = \Delta t_d \qquad \text{if } \Delta t_d < \Delta t_c$$

and the time step used to represent the dominant transport mechanism may have to be subdivided into a number of smaller time increments in comparison to the characteristic time for the weaker transport mode.

Computational procedure

The computational procedure is explained in the flowchart in *Figure 6*. Based on decomposition of the transport process into pure advection and pure diffusion, the proposed method consists of two steps re-

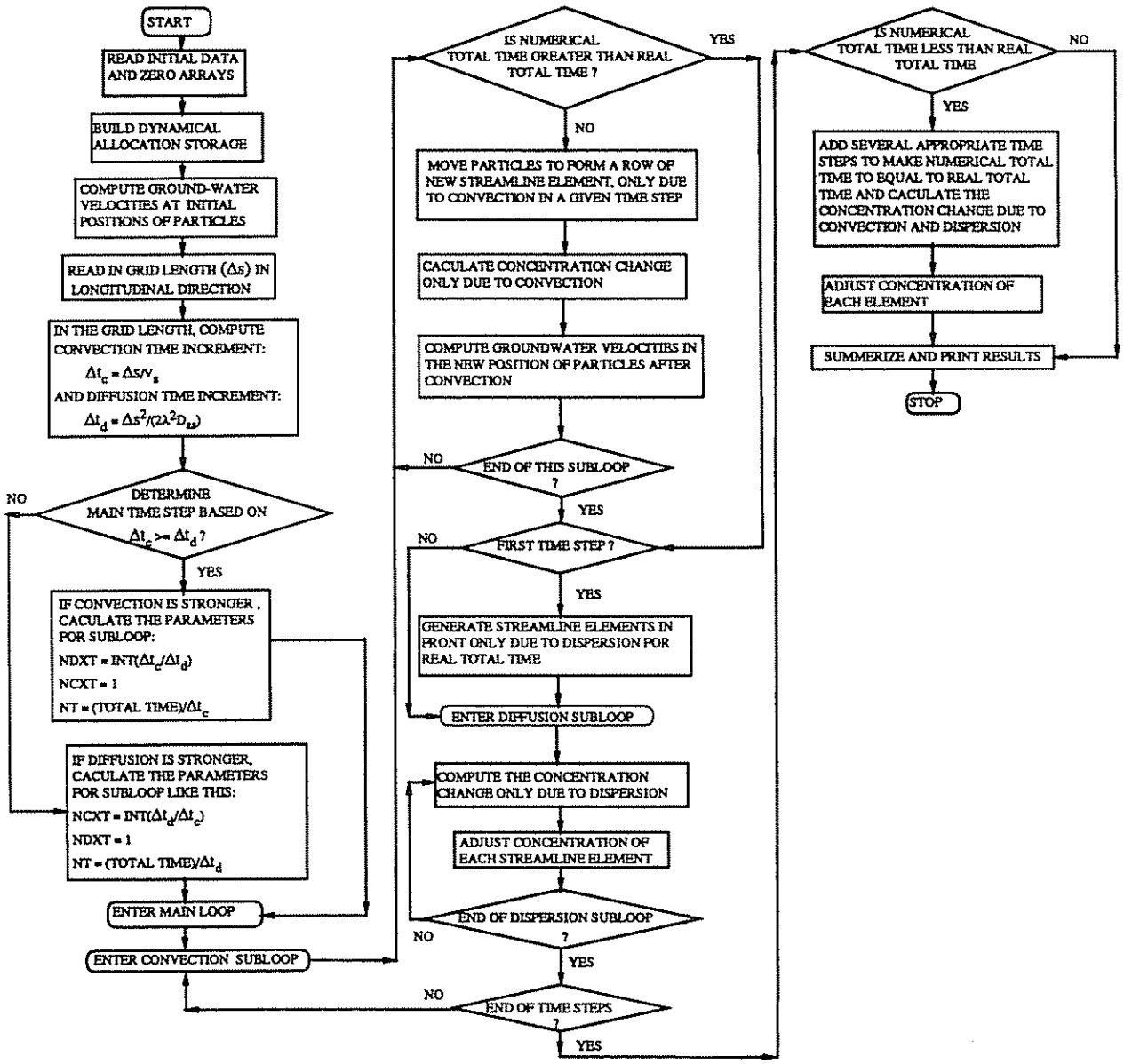

Figure 6. Flowchart illustrating the computational method

quiring the generation of a streamline element. If we assume, for clarity, that $\Delta t_d = \Delta t_c$, the procedure involves (1) first generating and moving particles caused by pure advection in the time increment Δt and defining

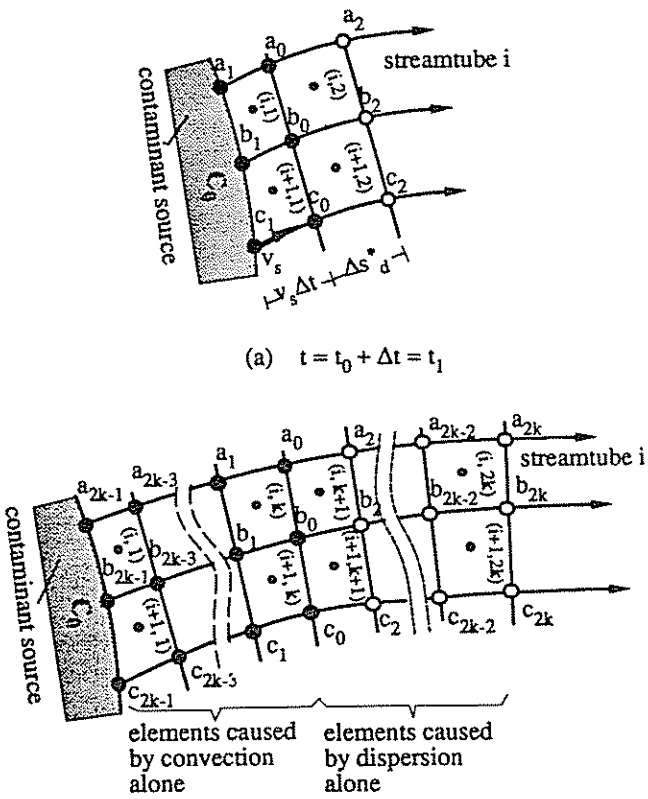

Figure 7. The development of advective and dispersive streamline elements

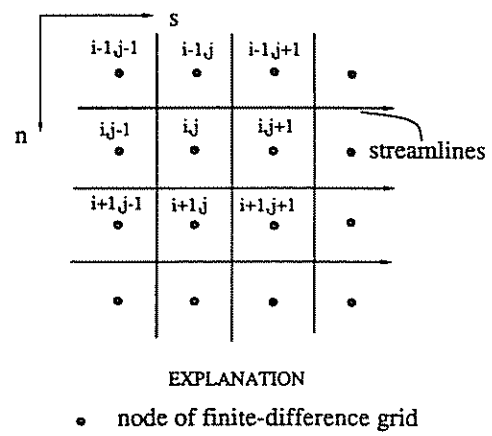

Figure 8. Finite difference grid

the streamline element by four adjacent characteristic particles and (2) then, ahead of the advective element, generating another streamline element caused by pure diffusion in the same time increment Δt.

By using (29) the location of particles a_2, b_2, and c_2 of *Figure 7(a)* may be defined and the appropriate streamline elements resulting from dispersion may also be identified. As illustrated in *Figure 7(a)*, there are two streamline elements generated in a streamtube from t_0 to t_1, for example, the element $a_1a_0b_0b_1$ generated by pure advection and the element $a_0a_2b_0b_2$ generated by pure diffusion beyond the front under consideration. In *Figure 7(b)*, even numbers and odd numbers are used to indicate the elements and particles caused by advection and diffusion, respectively. When $\Delta t_d = \Delta t_c$, two kinds of streamline elements are generated alternately with time to be symmetrical about the center line $a_0b_0c_0$.

The finite difference grid adopted in the procedure corresponds to that defined locally by the streamlines. The size and location of the cells in the grid vary in direct proportion to the sizes of the streamline elements. The total change in concentration in an aquifer is computed by solving (11) and (12). Equation (11), which is related to changes in concentration caused by advective transport alone, is solved by the movement of streamline elements as described previously. The changes in concentration caused by hydrodynamic dispersion, fluid sources, divergence of velocity, and changes in saturated thickness are calculated by using an explicit finite difference approximation (12), which can be expressed as

$$\Delta C_{i,j,k} = \Delta t\left[\frac{\partial}{\partial s}\left(D_{ss}\frac{\partial C}{\partial s}\right) + \frac{\partial}{\partial n}\left(D_{nn}\frac{\partial C}{\partial n}\right)\right] \tag{33}$$

As illustrated in *Figure 8*, the finite difference approximation of the longitudinal derivative may be expressed as

$$\frac{\partial}{\partial s}\left(D_{ss}\frac{\partial C}{\partial s}\right) = \left[\frac{D_{ss[i,j+1/2]}(C_{i,j+1} - C_{i,j})}{s_{i,j+1} - s_{i,j}} - \frac{D_{ss[i,j-1/2]}(C_{i,j} - C_{i,j-1})}{s_{i,j} - s_{i,j-1}}\right] \tag{34}$$

A finite difference approximation for the derivative in the n direction for equation (33) is developed for node (i,j) in an analogous manner as

$$\frac{\partial}{\partial n}\left(D_{nn}\frac{\partial C}{\partial n}\right) = \frac{D_{nn[i+1/2,j]}(C_{i+1,j} - C_{i,j})}{n_{i+1,j} - n_{i,j}} - \frac{D_{nn[i-1/2,j]}(C_{i,j} - C_{i-1,j})}{n_{i,j} - n_{i-1,j}} \tag{35}$$

Equation (33) is solved explicitly, and the element concentrations at the end of time increment k are computed as

$$C_{i,j,k} = C^*_{i,j,k} + \Delta C_{i,j,k} = C_{i,j-1,k-1} + \Delta C_{i,j,k} \tag{36}$$

Stability criteria

The explicit numerical solution of the diffusive transport equation requires that solution time steps do not violate the criteria of conditional stability.

For an explicit solution,[4]

$$\frac{D_{ss}\Delta t}{(\Delta s)^2} + \frac{D_{nn}\Delta t}{(\Delta n)^2} \leq \frac{1}{2} \tag{37}$$

Substituting the second relationship of (32) into (37) yields

$$\frac{\Delta s}{\Delta n} \leq \left[(\lambda^2 - 1)\frac{D_{ss}}{D_{nn}}\right]^{1/2} = \left[(\lambda^2 - 1)\frac{\alpha_L}{\alpha_T}\right]^{1/2} \tag{38}$$

If $\alpha_L = 0$, then $\Delta s/\Delta t \leq \infty$, and the explicit finite difference solution of (33) is stable for any Δs in longitudinal dispersion. Substitution of (32) into (37) gives

$$\left[\frac{\alpha_L}{\Delta s} + \frac{\Delta s \alpha_L}{(\Delta n)^2}\right] \leq \frac{1}{2} \tag{39}$$

and represents appropriate grid dimensions conditioned by stability constraints.

Validation

Analytical solutions to one- and two-dimensional transport geometries are used to compare the effectiveness of the adaptive model under Peclet numbers (Pe) ranging from zero to infinity. The results are reported in the following.

One-dimensional semi-infinite example

Transport is governed by the one-dimensional form of equation (1) under unidirectional flow in the x_i direction. The initial and boundary conditions are given by

$$\begin{aligned} C_0 &= 0 \quad & t &= 0 \\ C(0, t) &= 1 \quad & t &> 0 \\ C(\infty, t) &= 0 \quad & t &> 0 \end{aligned} \tag{40}$$

and the solution is well known as[17]

$$C(x, t) = \frac{1}{2}\left\{\operatorname{erfc}\left[\frac{x - vt}{2(Dt)^{0.5}}\right] + \exp\left[\frac{vx}{D}\right]\operatorname{erfc}\left[\frac{x + vt}{2(Dt)^{0.5}}\right]\right\} \tag{41}$$

The numerical calculations are completed for a finite domain of length $L = 10$ and height $H = 2$, illustrated in *Figure 9*. To compare transport behavior for different computational mesh sizes, the local Peclet number is defined as

$$\mathrm{Pe} = \frac{v\Delta s}{D_{ss}} \tag{42}$$

to indicate solution sensitivity to the relative importance of advective and dispersive transport. Four different Peclet numbers are used to represent the respective cases of dispersion dominant transport (Pe = 0.01), dispersive-advective transport (Pe = 1.0), advection dominant transport (Pe = 10), and pure advection (Pe = ∞). The length L and solution time t at which the results are displayed are chosen such that at all times between 0 and t the boundary condition given in (40) of $C(\infty, t)$ is reasonably satisfied at $x = L$.

The numerical and analytical solutions are presented in *Figures 10–13*. The numerical solutions reproduce the analytical results for all four cases without either oscillation close to the advective front or any apparent tendency for overshoot. This is particularly encouraging when compared with the results of Eulerian methods, which commonly exhibit poor correspondence for Pe > 10. Of particular note is the ability of the method to reproduce the analytical results exactly at Pe = ∞.

Comparison of three different grid sizes and three values of λ are completed for this one-dimensional transport example, as illustrated in *Figures 14* and *15*.

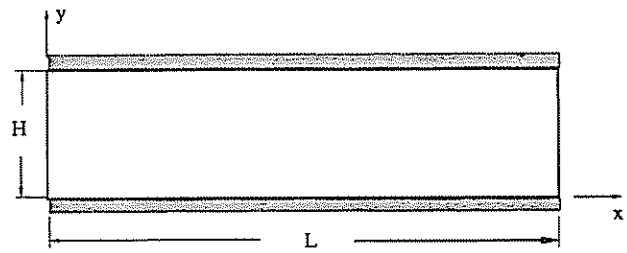

Figure 9. Physical domain for transport examples

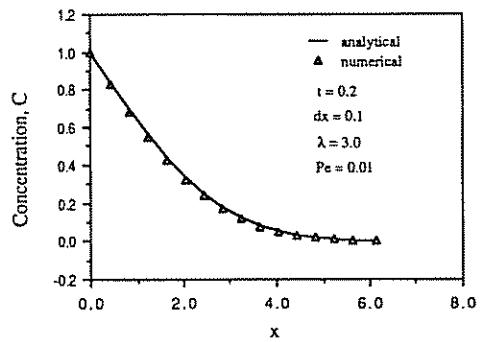

Figure 10. Concentration profile for one-dimensional semi-infinite example (Pe = 0.01)

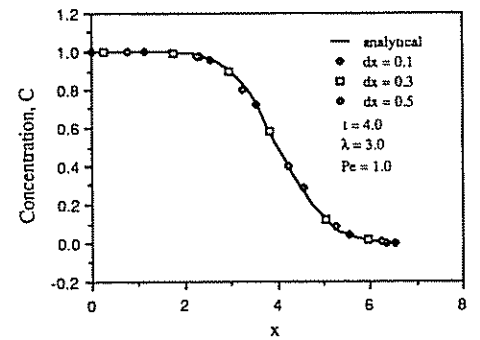

Figure 11. Concentration profile for one-dimensional semi-infinite example (Pe = 1.0)

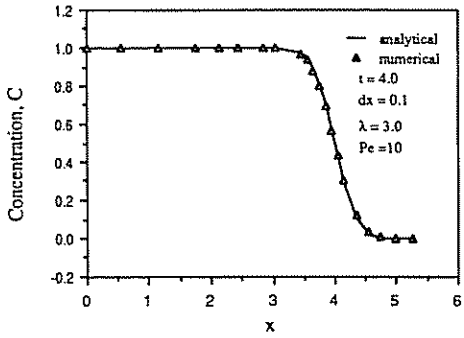

Figure 12. Concentration profile for one-dimensional semi-infinite example (Pe = 10)

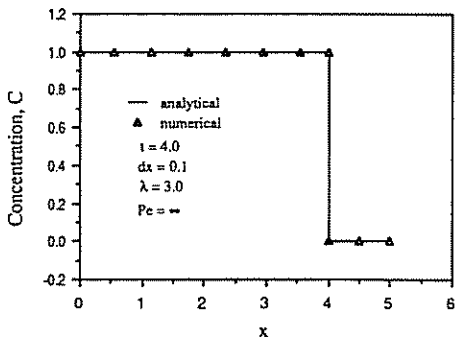

Figure 13. Concentration profile for one-dimensional semi-infinite example (Pe = ∞)

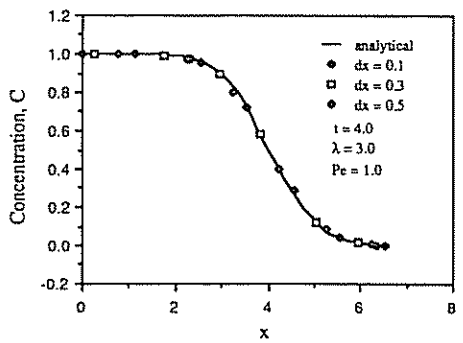

Figure 14. Grid dependence of the solution for the one-dimensional semi-infinite example

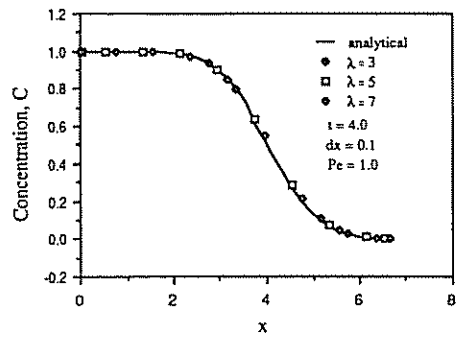

Figure 15. Solution dependence on the magnitude of λ for the one-dimensional semi-infinite example

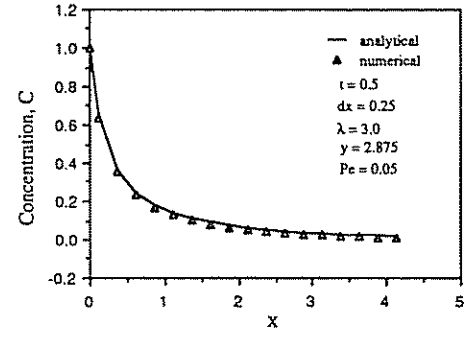

Figure 16. Concentration profile for two-dimensional semi-infinite example (Pe = 0.05)

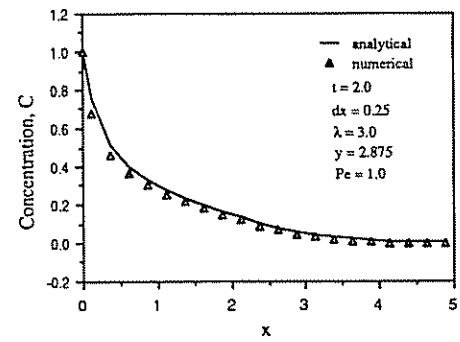

Figure 17. Concentration profile for two-dimensional semi-infinite example (Pe = 1.0)

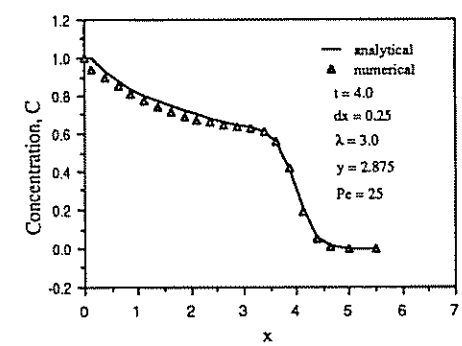

Figure 18. Concentration profile for two-dimensional semi-infinite example (Pe = 25)

Results indicate the absence of numerical diffusion in these cases provided that the domain grid meets the stability criteria of (38)–(39) and the value of λ is appropriately chosen in (27) to yield satisfactory numerical precision. Numerical precision may be enhanced by reducing grid size and simultaneously using a large magnitude of λ. However, a considerable computational penalty is engendered in this choice.

Two-dimensional semi-infinite example

Solution for advective-dispersive transport resulting from a finite source in a one-dimensional velocity field with longitudinal and transverse dispersion[18] is used to validate the solution for the two-dimensional case. The

boundary conditions are given by

$$C(0, y, t) = 1.0 \qquad 2 \leq y \leq 3$$
$$C(0, y, t) = 0 \qquad 2 > y > 3$$

All simulations are completed for a 10×5 aquifer whose lower half is shown in *Figure 9*, utilizing the inherent symmetry of the domain ($L = 10$, $H = 2.5$). In this example the three transport cases of dispersion-dominated transport (Pe = 0.05), dispersive-advective transport (Pe = 1.0), and advection-dominated transport (Pe = 25) are examined.

The numerical and analytical solutions are presented along the axis $y = 2.875$ in *Figures 16* through *18*. The results illustrate strong correspondence with the analytical results even for the high Peclet numbers reported in *Figure 18*.

Conclusions

An adaptive characteristics method is presented that is capable of effectively representing mixed diffusive-advective transport processes in porous media. Results remain satisfactory over a broad range of Peclet numbers, including those representing strongly advective flows. Spurious undershoot, overshoot, and oscillations around the advective front are not evident, and the absence of numerical diffusion is also encouraging in comparison with results traditionally obtained from Eulerian methods.

References

1 Christie, I. et al. Finite element methods for second order differential equations with significant first derivatives. *Int. J. Num. Meth. Eng.* 1976, **10**, 1389–1396

2 Garder, A. O., Peaceman, D. W., and Pozzi, A. L. Numerical calculation of multi-dimensional miscible displacement by the method of characteristics. *Soc. Petr. Eng. J.* 1964, **4**, 26–36

3 Pinder, G. F. and Cooper, H. H. A numerical technique for calculating the transient position of the salt water front. *Water Resour. Res.* 1970, **6**, 875–882

4 Reddell, D. L. and Sunada, D. K. Numerical simulation of dispersion in groundwater aquifers. Hydrol. Paper 41, Colorado State University, Fort Collins, CO, 1970

5 Bredehoeft, J. D. and Pinder, G. F. Mass transport in flowing groundwater. *Water Resour. Res.* 1973, **9**, 192–210

6 Neuman, S. P. A Eulerian-Lagrangian numerical scheme for the dispersion-convection equation using conjugate space-time grids. *J. Comp. Phys.* 1981, **41**(2), 270–294

7 Neuman, S. P. Adaptive Eulerian-Lagrangian finite element method for advection-dispersion. *Int. J. Num. Meth. Eng.* 1984, **20**, 321–337

8 Benque, J. P., Ibler, B., Keramsi, A., and Labadie, G. A finite method for Navier-Stokes equations. *Proceedings of the Third International Conference* on Finite Elements in Flow Problems, Banff, Alberta, Canada, 1980

9 Pironneau, O. On the transport diffusion algorithm and its application to the Navier-Stokes equations. *Numer. Math.* 1982, **38**, 309–332

10 Hasbani, Y., Livne, E., and Bercovier, M. Finite elements and characteristics applied to advection diffusion equations. *Computers and Fluids* 1983, **11**(2), 71–83

11 Hervouet, J. M. Application of the method of characteristics in their weak formulation to solving two-dimensional advection equations on mesh grids. *Computational Techniques for Fluid Flow*, ed. C. Taylor, J. A. Johnson, and W. R. Smith, Pineridge Press, Swansea, UK, 1986, 149–185

12 Scheiddeger, A. E. General theory of dispersion in porous media. *J. Geophys. Res.* 1961, **66**(10), 3273–3278

13 Aris, R. *Vectors, Tensors and the Basic Equations of Fluid Mechanics*. Prentice-Hall, Englewood Cliffs, N.J., 1962, p. 286

14 Konikow, L. F. and Bredehoeft, J. D. Computer model of two-dimensional solute transport and dispersion in groundwater. *U.S. Geol. Surv.* 1978 7(2)

15 Elsworth, D. A boundary element–finite element procedure for porous and fractured media flow. *Water Resour. Res.* 1987, **23**(4), 551–560

16 Bear, J. *Hydraulics of Groundwater*. McGraw Hill, New York, 1979, p. 569

17 Ogata, A. and Banks, R. B. A solution to the differential equation of longitudinal dispersion in porous media. Professional Paper 411-A, U.S. Geological Survey, Washington, D.C., 1961, p. 7

18 Cleary, R. W. Groundwater pollution and hydrology: Mathematical models and computer programs. Report 78-WR-15, Water Resources Program, Princeton University, Princeton, N.J., 1978